Interannual Variability of the Antarctic Ozone Hole in a GCM. Part II: A Comparison of Unforced and QBO-Induced Variability

DREW T. SHINDELL, DAVID RIND, AND NAMBATH BALACHANDRAN

NASA/Goddard Institute for Space Studies, and
Center for Climate Systems Research, Columbia University, New York, New York

(Manuscript received 20 January 1998, in final form 5 August 1998)

ABSTRACT

Simulations were performed with the Goddard Institute for Space Studies GCM including a prescribed quasi-biennial oscillation (QBO), applied at a constant maximum value, and a physically realistic parameterization of the heterogeneous chemistry responsible for severe polar ozone loss. While the QBO is primarily a stratospheric phenomenon, in this model the QBO modulates the amount and propagation of planetary wave energy in the troposphere as well as in the stratosphere. Dynamical activity is greater in the easterly than in the unforced case, while westerly years are dynamically more quiescent. By altering zonal winds and potential vorticity, the QBO forcing changes the refraction of planetary waves beginning in midwinter, causing the lower-stratospheric zonal average temperatures at Southern Hemisphere high latitudes to be ~3–5 K warmer in the easterly phase than in the westerly during the late winter and early spring. Ozone loss varies nonlinearly with temperature, due to the sharp threshold for formation of heterogeneous chemistry surfaces, so that the mean daily total mass of ozone depleted in this region during September was 8.7×10^{10} kg in the QBO easterly maximum, as compared with 12.0×10^{10} kg in the westerly maximum and 10.3×10^{10} kg in the unforced case. Through this mechanism, the midwinter divergence of the Eliassen–Palm flux is well correlated with the subsequent springtime total ozone loss ($R^2 = 0.6$). The chemical ozone loss differences are much larger than QBO-induced transport differences in our model.

Inclusion of the QBO forcing also increased the maximum variability in total ozone loss from the ~20% value found in the unforced runs to ~50%. These large variations in ozone depletion are very similar in size to the largest observed variations in the severity of the ozone hole. The results suggest that both random variability and periodic QBO forcing are important components, perhaps explaining some of the difficulties encountered in previous attempts to correlate the severity of the ozone hole with the QBO phase.

1. Introduction

The ozone hole over Antarctica highlights the extent to which human activities can disrupt our environment. Observations show that more than 50% of the ozone layer has been destroyed over the entire Antarctic region each spring in recent years (e.g., McPeters et al. 1996). The ozone hole leads to significant increases in surface ultraviolet radiation and, through dilution, may also affect the midlatitude ozone layer (e.g., Cariolle et al. 1990; Prather and Jaffe 1990). Furthermore, recent model simulations indicate that severe depletion may be worsened, and eventual recovery delayed, by greenhouse gas increases (Shindell et al. 1998a; Dameris et al. 1998). As such, it is important to understand the factors that govern the formation of the ozone hole and those that determine its interannual variability.

The heterogeneous halogen chemistry that destroys ozone is extremely sensitive to temperature, so that changes of only a few degrees can have a significant impact on total ozone depletion. In the isolated air trapped within the polar vortex, temperatures become so low during the austral winter and spring that polar stratospheric clouds (PSCs) or supercooled ternary solution (STS) droplets can form. Reactions on the particle or droplet surfaces are capable of rapidly converting chlorine from reservoir species into active forms that destroy ozone (e.g., World Meteorological Organization 1994). The formation of these surfaces is nonlinearly dependent on temperature, with typical temperatures in the springtime lower stratosphere within the southern vortex falling very near the critical threshold values, so that the degree of chlorine activation can be strongly influenced by small temperature variations induced by any mechanism. In Part I of this study (Shindell et al. 1997; hereafter referred to as Part I), we suggested that random, unforced interannual variability [without including the effects of the quasi-biennial oscillation (QBO) in the model] in the propagation of tropospheric wave energy into the stratosphere played a significant role in modulating temperatures, and therefore in influencing the severity of the Antarctic ozone hole.

Corresponding author address: Dr. Drew T. Shindell, NASA/GISS, Columbia University, 2880 Broadway, New York, NY 10025.
E-mail: dshindell@giss.nasa.gov

The QBO also plays an important role in interannual variability and is expected to cause temperature changes in the polar lower stratosphere (e.g., Balachandran and Rind 1995). Several previous studies have examined the possible correlation between observations of the severity of the ozone hole and the QBO (Garcia and Solomon 1987; Lait et al. 1989; Gray and Ruth 1993; Bodeker and Scourfield 1995). However, variability in the real atmosphere may be influenced by the irregularity in the period of the QBO and by the interaction between the QBO and the annual cycle, as well as by random variability in the atmosphere. The combination of these factors has made it difficult to unravel the influence of the individual components on ozone depletion.

To isolate the impact of the QBO on polar ozone loss, our experiments simulate the idealized situation where the QBO is applied as a fixed forcing, so that the irregular component of QBO variability and the interaction between the QBO and the annual cycle are not involved. We have performed model simulations with the Goddard Institute for Space Studies (GISS) Global Climate Middle Atmosphere Model (GCMAM) including the QBO forcing. Though computationally expensive, it is necessary to use a three-dimensional model, such as this, which solves the primitive equations and includes a complete stratosphere to correctly simulate planetary wave propagation.

Part I of this study showed that random variability in midwinter generation of tropospheric wave energy played an important role in determining its later propagation in the stratosphere, and hence on the severity of the Antarctic ozone hole. Modeled interannual variability in the springtime ozone hole due solely to variability arising from random forcing was shown to be of the same order of magnitude as, though smaller than, the observed variability. We now investigate how the QBO influence on wave propagation and temperatures seen in our previous experiments (Balachandran and Rind 1995) affects the Antarctic ozone hole and compare the variability induced by the QBO forcing with the ''unforced'' case and with observations.

2. Model design

The experimental setup and chemistry parameterizations were described in detail in Part I of this series. In brief, a physically realistic parameterization of the polar stratospheric heterogeneous chemistry responsible for the Antarctic ozone hole was included online in the GISS GCMAM (Rind et al. 1988a,b). A gravity wave parameterization is employed in which the model temperature and wind fields in each grid box are used to calculate gravity wave effects due to wind shear, convection, and topography. The model version used has 23 vertical layers, extending from the surface to 85 km, with $8^\circ \times 10^\circ$ (latitude $\times$ longitude) horizontal grid spacing. For these experiments, the mountain drag was set to one-quarter the amount used in the initial studies (Rind et al. 1988a,b), a standard modification used in all of our studies of polar ozone (Shindell et al. 1997, 1998a,b). As in the earlier simulations, the residual circulation and the generation of planetary waves in the altered model are in fairly good agreement with observations. The altered model now gives a good reproduction of observed temperatures in the southern polar lower stratosphere during the austral winter and spring, which were otherwise too warm. Reducing the drag does marginally reduce the variability in the model, as well as slightly degrade the simulation at other seasons and latitudes, however.

The GISS GCMAM does not generate a QBO, most likely as a result of insufficient resolution. This is a common difficulty in GCMs (e.g., Hamilton 1995). We have forced a QBO in the model by setting the equatorial winds equal to the peak values observed for the easterly and westerly phases of the QBO, initialized with a time constant of 30 days, as in Balachandran and Rind (1995). Specifically, the winds in the layers centered at 31.6 and 14.7 mb were forced to -25 m s^{-1} for the easterly phase and $+25$ m s^{-1} for the westerly phase, with an exponential falloff away from these heights and away from the equator. The forcing extends in effect from 20 to 40 km altitude and from 27°S to 27°N. The model gravity wave drag and Eliassen–Palm (EP) flux divergence response generates an oppositely directed wind above the forcing at around the 2-mb level at the equator. The resulting overall wind field is in good agreement with observations. The QBO forcing in our model does not vary with time as it does in the real atmosphere, however. We have chosen to force the QBO at a maximum in each phase to explore the effects of a strong, constant equatorial wind. Though we reduce the realism of the simulation, we greatly simplify the interpretation of the results and are able to more clearly isolate the influence of the QBO from the random, unforced variability of the model. This method avoids the numerous difficulties that have been encountered in attempts to derive a correlation between ozone hole severity and a QBO varying quasi-regularly with time and altitude.

Chlorine activation is calculated in each grid box, with total chlorine in the model set to 3.2 parts per billion by volume (ppbv), corresponding to abundances of the early 1990s. Whenever temperatures fall below 195 K, a rough threshold for PSC or STS formation (there is little dependence on surface details; Jaeglé et al. 1997), full activation takes place in 5 h, as the heterogeneous reactions are very rapid even for very small surface areas (Shindell and de Zafra 1997). When heterogeneous processing ceases, deactivation follows model-derived latitude and altitude dependent rates for a denitrified vortex (Shindell and de Zafra 1997). Ozone depletion takes place at each point in the GCM where there is both active chlorine and sunlight, which is required for the chlorine catalytic cycle of ozone destruction. We also include an additional estimated contri-

bution of 15% from bromine chemistry, as seen in the offline chemical model. Ozone recovery rates are parameterized so that ozone losses are restored based on the photochemical lifetime of ozone at each altitude.

Fixed climatological transport of ozone was used online due to limitations imposed by available computer resources. This includes only zonal mean motions (represented by transformed Eulerian means), so that we may slightly underestimate the amount of air chemically processed by longitudinally asymmetric motion of parcels into and out of low-temperature regions. Since we are concerned with Southern Hemisphere springtime ozone loss, which is generally well confined within the strong polar vortex, this should not greatly influence our results. Changes in ozone transport between the QBO phases were calculated offline and did not interact with radiation, according to our standard method, which computes the product of the horizontal and vertical transports and the ozone gradients in each direction, including both mean and eddy-forcing effects (Shindell et al. 1998b). All values in this paper include the total chemistry-plus-transport ozone change unless otherwise specified.

The GCMAM was run for 10 model years for each phase of the QBO forcing. Additionally, the model simulation without any QBO forcing that was reported on in Part I was extended to 10 yr to facilitate comparisons.

3. The correlation between QBO and ozone hole severity

Several studies have investigated the possible correlation between the severity of the ozone hole and the QBO since an apparent quasi-biennial periodicity in ozone losses in the early eighties was first noted (Bojkov 1986; Stolarski et al. 1986). Though the observational relationship between QBO phase and ozone loss has been extensively examined, the conclusions are difficult to interpret, largely because of the lack of agreement in defining the phase of the QBO. For example, based on the September 30-mb winds, strong variations in ozone seen between 1986, 1987, and 1988 are well correlated with the phase of the QBO. However, the correlation with 30-mb winds is less clear for 1989, 1992, and 1993. Garcia and Solomon (1987) used the equatorial wind speed at 50 mb during October. Lait et al. (1989) used the August–September average of both 50- and 30-mb equatorial winds and found a higher correlation between ozone loss and the 30-mb winds. After a detailed study of the relationship between various QBO parameters and ozone loss, Gray and Ruth (1993) concluded that there is not a unique variable such as wind at a particular level during a particular month that can be definitively correlated with the severity of the ozone hole because of complications such as the irregular descent rate of the QBO phase and the time of year at which the phase changes. Bodeker and Scourfield (1995) again correlated the strength of the ozone hole with 30-mb winds, but phase shifted by +12 months, and asserted that there was a strong correlation.

Observations of the QBO and the ozone hole are shown in Fig. 1. The top two panels show equatorial winds at 30 and 50 mb from Canton Island (2.5°S, 171.4°W), the Maldives (0.4°S, 73.1°E), and Singapore (1.2°N, 103.6°E) as compiled at the Free University, Berlin (Naujokat 1986), updated through 1995 (S. Pawson 1997, personal communication). The bottom panel shows total depleted ozone mass averaged over the Antarctic vortex period (19 July–1 December), calculated by summing the depletion at all points with less than 220 Dobson units (DU) relative to the 220-DU threshold, according to the technique given in Bodeker and Scourfield (1995), but using revised Total Ozone Mapping Spectrometer (TOMS) version 7 data (G. Bodeker 1997, personal communication). While observations do suggest some periodicity in ozone hole severity, a definitive correlation with the QBO remains tantalizingly elusive.

The exact physical mechanism linking the equatorial QBO to high-latitude temperatures and ozone is also not completely clear. It seems likely that the position of the zero wind surface in the subtropics, which is modulated by the QBO, itself modulates extratropical planetary wave refraction (Holton and Tan 1980). Or perhaps changes in the extratropical zonal wind in the middle and upper stratosphere are responsible for deflecting planetary waves (Kodera 1991). Whatever the mechanism, during an easterly phase QBO, a dynamically active year is expected with greater refraction of wave energy to high latitudes, leading to a weaker polar vortex and a greater transfer of heat to the polar regions than in the westerly phase (Hamilton 1989; Dunkerton and Baldwin 1991). The resulting temperature differences in the polar lower stratosphere between the two QBO phases could significantly affect the extremely nonlinearly temperature-dependent heterogeneous chemistry responsible for the ozone hole.

Additionally, there will be a modulation of high-latitude ozone amounts due to a QBO in ozone transport. Examining column ozone anomalies during the 1970s from Nimbus 4 BUV data, Hasebe (1983) found a maximum QBO effect of about 6 DU in the Southern Hemisphere. Nimbus 7 data from 1979 to 1982, safely before the onset of severe polar ozone depletion, also shows a maximum QBO modulation of high-latitude column ozone of 6 DU in the Southern Hemisphere (Lait et al. 1989). Since these variations include QBO modulation of both transport and chemistry, the effect of the QBO on ozone transport alone is likely a minor one and too small to account for the observed variation in the severity of the ozone hole.

The QBO modulation of temperature should lead to a greater amount of ozone loss at high latitudes in the colder, less active westerly phase. However, variability in tropospheric wave activity unrelated to the QBO can also affect temperatures in the polar lower stratosphere,

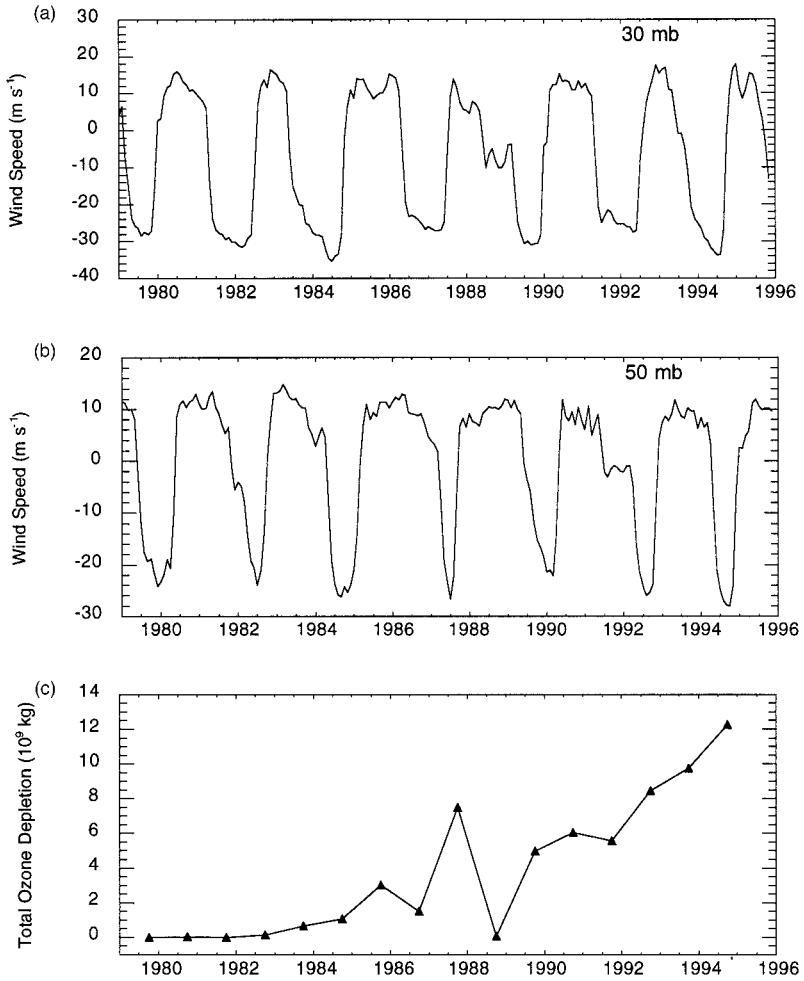

FIG. 1. The top two panels show observed equatorial winds at 30 and 50 mb, respectively, from Canton Island (2.5°S, 171.4°W), the Maldives (0.4°S, 73.1°E), and Singapore (1.2°N, 103.6°E) as compiled at the Free University, Berlin (Naujokat 1986). The bottom panel shows total depleted ozone mass averaged over 19 Jul–1 Dec (G. Bodeker 1997, personal communication)

as shown in Part I. Furthermore, solar variability and the 1991 eruption of Mt. Pinatubo also likely influenced the ozone hole. Given the difficulties associated with a complicated forcing, we believe that it is useful to study the idealized situation where the QBO is applied as a fixed forcing to isolate the QBO influence on wave activity and propagation and the resulting impacts on polar ozone depletion. We hope this modeling work may help in understanding the observed variability.

4. Temperature response to the QBO

The modeled temperature variations induced by the QBO are shown in Fig. 2, given as the difference between easterly and westerly phase zonal average temperatures in the GCMAM. As expected, the east winds cause colder temperatures in the equatorial lower stratosphere, with warmer temperatures above. At extratropical latitudes, the lower stratosphere is consistently warmer in the easterly phase, consistent with the increased refraction of wave energy and transfer of heat to higher latitudes associated with this phase. The general pattern is similar to that found in Balachandran and Rind (1995) and is qualitatively similar to the National Meteorological Center [NMC; now the National Centers for Environmental Prediction (NCEP)] data shown therein. Ozone hole formation is strongly influenced by temperatures in the southern polar lower stratosphere during the austral winter and spring. The temperature differences there are among the largest found in our experiments, with easterly minus westerly differences of up to 6° during September–November (austral spring). The observed differences are up to 9° (Balachandran and Rind 1995), but these depend upon the positive feedback of ozone depletion, so it is more difficult to isolate the signal of the QBO alone. Earlier in

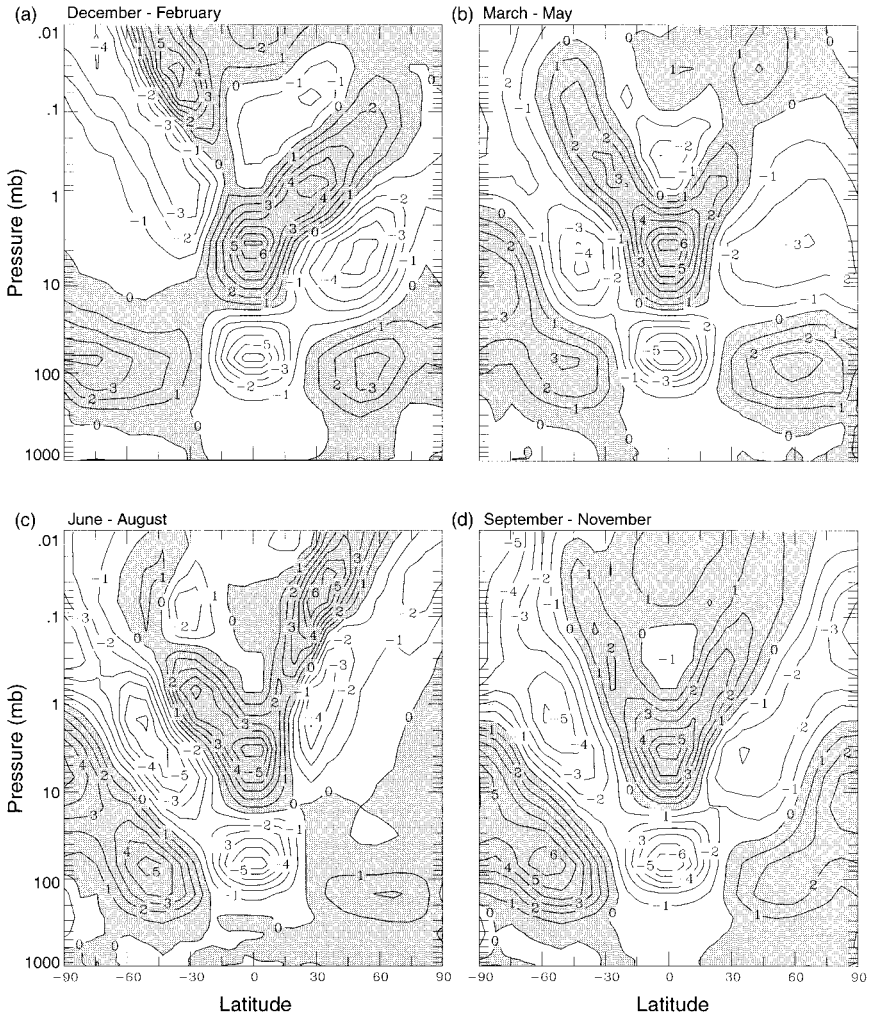

FIG. 2. Zonal mean temperature differences between the QBO easterly and westerly phases (in K). Values are differences (easterly minus westerly) between the averages of the 10-yr runs done with each phase of the QBO forcing. Positive values are shaded.

the winter, before the onset of ozone depletion, the modeled June–August temperature changes of 3–5 K are consistent with observed interannual variability (e.g., Randel 1987; NCEP data), though at the high end, as expected since our applied forcing is a constant maximum value. Table 1 gives the zonal average temperatures at high southern latitudes during the austral winter and spring months at 32 mb, where differences induced by the QBO are quite large. Zonal average differences of 4° are typical during the key month of September, when continuous heterogeneous chlorine activation is crucial for maintaining rapid ozone depletion rates. Since the temperatures are near the 195 K threshold for PSC or STS formation, these relatively small temperature differences can greatly affect ozone loss rates.

TABLE 1. Zonal average temperatures at 32 mb (in K).

Latitude	July	August	September	October
		Westerly phase		
63°–71°S	198	196	199	207
71°–79°S	193	192	194	202
79°–87°S	190	189	191	197
		Easterly phase		
63°–71°S	201	199	203	214
71°–79°S	195	194	198	208
79°–87°S	192	190	193	204

The temperature response to the QBO is somewhat larger than that given in Balachandran and Rind (1995) for similar QBO forcing, but without ozone change. In the earlier experiment, the maximum easterly minus westerly zonal average temperature difference in the southern lower stratosphere during September–November was 3 K, versus the 6 K shown in Fig. 2. The cooling in the upper stratosphere has also increased, from −3 to −5 K with the presence of the ozone hole. This enhanced temperature response is consistent with the expected impacts of the ozone hole, which causes ra-

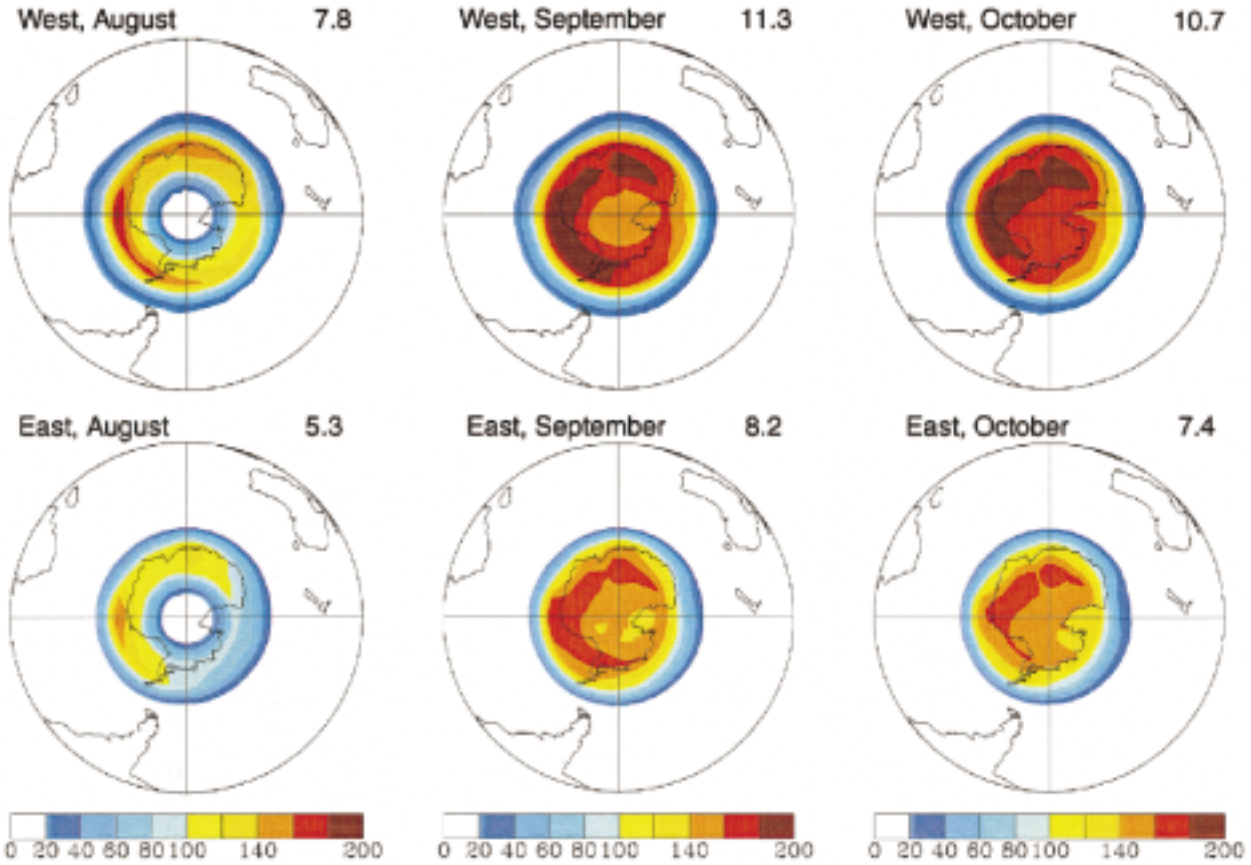

FIG. 3. Total column ozone loss (DU) in the GCM during the ozone hole period of August, September, and October. Results are averages of the 10-yr runs done with each phase of the QBO forcing. The number in the upper-right corner of each map is the global average loss, which is useful for comparison of losses in the two phases.

diative cooling in the lower stratosphere and dynamical heating in the upper stratosphere, as seen in Part I. Since the ozone depletion is greater in the westerly phase, as discussed below, these impacts should be larger in the westerly than in the easterly phase, resulting in the positive feedback on temperature seen in these experiments.

5. Ozone response to QBO

Ozone loss rates respond to the temperature differences between the QBO phases based on the heterogeneous chemistry parameterization. Total column ozone depletion in the GCM during the period of ozone hole formation is shown averaged over the 10 yr of each model run in Fig. 3. These values include differences in ozone transport relative to the control run, as calculated noninteractively. Ozone losses are 37% and 44% greater in the westerly phase than in the easterly phase during September and October, respectively. The horizontal extent of the ozone hole is also greater during the westerly QBO phase, with losses of 20 DU reaching the southern tip of South America, while in the easterly phase the 20-DU contour is estimated to be several degrees farther south, roughly halfway between the tip of South America and the end of the Antarctic peninsula. Zonally averaged vertical profiles of ozone depletion during September for each QBO phase and the control run, along with the difference, are shown in Fig. 4. The QBO clearly extends the vertical and horizontal extent of the ozone hole. An interesting feature is the small region in the lowermost stratosphere where there is actually more depletion in the easterly phase than in the westerly phase. This difference seems to result from greater wave-induced displacement of the polar vortex in the more active easterly phase, which exposes low-temperature air parcels to sunlight earlier than occurs in the more quiescent westerly phase.

We also find that the QBO increases the duration of the ozone hole, with longer lasting depletion in the westerly phase. Similar results were seen in Part I, where the variability in tropospheric wave energy was shown to modulate the vertical and horizontal extent of ozone losses in the model. Of course the depletion is nearly complete in the heart of the ozone hole at the highest latitudes, so that no further loss is possible. At reduced chlorine levels that will occur over the next few decades, this saturation effect would not occur, and the QBO may then affect the amount of ozone depletion there as well.

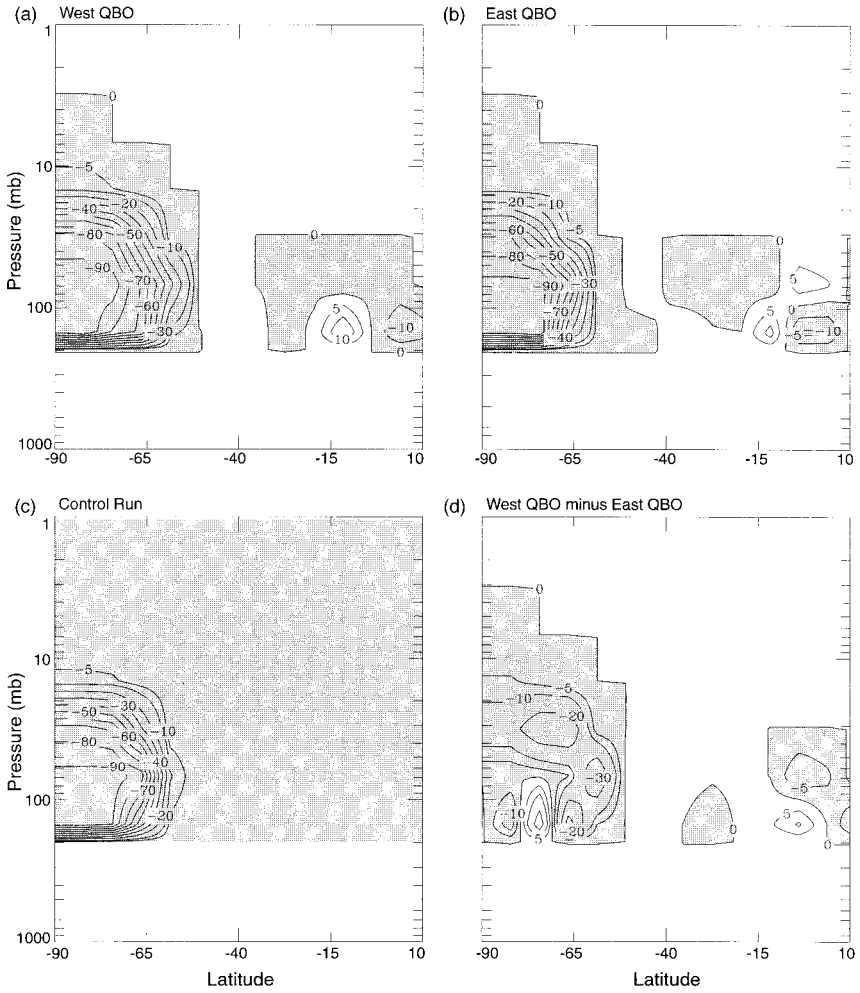

FIG. 4. Zonal mean percentage ozone change during Sep for the average of the 10-yr runs done with each phase of the QBO forcing, and the difference between the two phases, along with the unforced control case. Losses are shaded, except in the difference panel, where negative values indicate greater ozone depletion in the westerly phase. Note that the transport effects shown here are changes relative to the control, so that there were no transport changes in the control case by definition.

The effects of transport are most clearly seen in the modulation of lower-stratospheric ozone near the equator. Transport also plays a role in the high-latitude response, with enhanced descent in the easterly QBO phase relative to the westerly. This results in a relative ozone decrease in the westerly phase, which adds on to the greater chemical depletion to create the large negative values seen in the westerly minus easterly differences shown in Fig. 4. Greater transport of ozone to the polar regions during the QBO easterly phase was also simulated in the model of Hess and O'Sullivan (1995). The largest effects of transport are approximately 10% in our model for any particular zonal mean value, while the mean total ozone change over all area due to altered transport is only about 5% of the mean chemical change.

TABLE 2. Total depleted ozone mass ($\times 10^{10}$ kg), Sep daily average, Jul Southern Hemisphere tropospheric kinetic energy in wave 1 ($\times 10^{17}$ J), and Jul zonal wind forcing by EP flux divergence ($\times 10^{-6}$ m s^{-2}) from 10 to 150 mb, 23°–55°S. Standard deviation is σ. All values are averages over each 10-yr run.

Forcing	Mean ozone loss	σ	Mean wave energy	σ	dU by EP flux divergence	σ
QBO easterly phase	8.7	0.95	338	32	2.4	1.6
None	10.3	0.92	307	39	1.1	1.2
QBO westerly phase	12.0	0.93	290	27	−0.3	1.9

Table 2 lists the mean and standard deviation in daily total depleted ozone mass for both QBO phases, along with values for the unforced run, all for September. For comparison with the TOMS data shown in Fig 1, the daily means were also averaged over August–November including only model points at latitudes from 40° to 70°S

and with column ozone less than 220 DU, as in the analysis of the TOMS data. This reduces the depleted ozone mass by more than an order of magnitude, with roughly a factor of 4 coming from each of the lack of data from 70° to 90°S and the arbitrary 220-DU limit. Using this procedure, the values of total depleted ozone mass are 9.7×10^9, 7.4×10^9, and 3.6×10^9 kg for the QBO westerly, unforced, and QBO easterly cases, respectively. A comparison of these values to the totals given in Table 2 shows that the percentage variability is much larger when the model is sampled to match the satellite observations. This is likely due to the greatest variability in the magnitude and duration of ozone losses occurring at the edges of the ozone hole, and suggests that the TOMS sampling may exaggerate the variability of the ozone hole.

Based on the total ozone depletion in the model (as in Table 2), the QBO forcing alters the mean loss by ±16% versus the unforced mean. The standard deviation within each case is quite similar, showing that the addition of either phase of the QBO forcing does not alter the range of ozone losses so much as offset them from the unforced case. The difference in mean ozone loss between the QBO phases, 3.3×10^{10} kg, is considerably greater than the variability within each case of $\sim 1 \times 10^{10}$ kg. QBO forcing thus has a greater influence on ozone loss than does natural variability in our model when the QBO forcing is at its maximum. In the real atmosphere, the variation of the QBO phase with time and its interaction with the annual cycle would likely lead to variations in the effectiveness of the QBO in modulating the level of and propagation of planetary wave activity during the midwinter and spring months, however. One would therefore expect a time-varying QBO forcing to lead to ozone losses anywhere between the unforced case and the maxima calculated here.

In the unforced run, the standard deviation in total ozone depletion averaged in the same manner as the data over August–November was 1.2×10^9 kg, with a maximum variability of 3.3×10^9 kg. When the QBO forcing was applied, the maximum variability increased to 9.8×10^9 kg. Since the QBO forcing was a constant maximum, the standard deviation is not suitable for comparison. Observations also show a large maximum variability, with changes in total depleted ozone of 7.4×10^9 kg between 1987, 1988, and 1989, as shown in Fig. 1. Observations seem to indicate a larger value of typical variability than the 1.2×10^9 kg seen in our unforced run, though this is difficult to assess given the steadily increasing amount of chlorine in the atmosphere. Certainly it seems that unforced variability alone cannot account for the largest variations seen in observations, while ozone loss differences due to the maximum QBO forcing are much closer to the maximum observed variations. Our model results do suggest that unforced variability is an important component however, contributing roughly one-third of the variability in ozone hole severity, while the QBO contributes roughly two-thirds. Thus we would expect difficulties in any attempts to correlate the severity of the ozone hole with the QBO phase due to the significant variability associated with effects other than the QBO.

6. QBO modulation of planetary waves

We now turn to the mechanism by which the equatorial QBO influences high-latitude temperatures. As described in Part I, the temperature variations in the lower stratosphere that modulate the rate of heterogeneous chemistry can be caused by variations in tropospheric wave energy forcing. The amount of wave energy deposited in the high-latitude lower stratosphere will depend upon both the amount of wave energy generated in the troposphere and on its propagation. The mean Southern Hemisphere tropospheric kinetic energy in wave 1 is given in Table 2 for the QBO easterly and westerly forcings, as well as the unforced case. In July, there is more wave energy in the easterly phase years than in the westerly phase years, with the unforced years falling approximately in the middle. As seen in Table 1, temperature differences are in fact apparent as early as July. The variability of wave energy within each run is fairly large however, so that the mean values in both QBO phases fall within one standard deviation from the mean seen in the unforced run.

The changes in the propagation of planetary waves are more significant. As expected, the poleward and upward fluxes are both greater in the easterly phase than in the westerly phase. We interpret the altered propagation as resulting from a refractive index response to the zonal wind and potential vorticity gradient changes induced by the QBO, as discussed in detail in Balachandran and Rind (1995). The winds in the equatorial stratosphere are, of course, opposite in the two QBO phases, as shown in Fig. 5. The easterly QBO increases the midlatitude meridional gradient of quasigeostrophic potential vorticity, shown in Fig. 6, because the horizontal wind shear is stronger at lower midlatitudes in the easterly phase, and there is also an increase in the vertical shear of the zonal wind. (Note that the observed quasigeostrophic potential vorticity gradient shows a qualitatively similar July pattern, with two main maxima located at around 200 mb, 20°–30°S, and above about 50 mb at 60°S (Randel 1987), but has a larger gradient in the vicinity of the subtropical jet and a smaller stratospheric gradient. However, the use of quasigeostrophic diagnostics in a primitive equation model introduces significant errors. Nevertheless, the correct location of the maxima should allow the model to correctly locate regions where wave propagation is favorable.) Planetary waves coming out of the troposphere, where westerly winds predominate, which are moving toward the equatorial stratosphere during an easterly QBO phase, are refracted and propagate poleward away from the subtropical zero wind line, as suggested by Holton and Tan (1980) and seen in the analyses of Kodera (1991). At

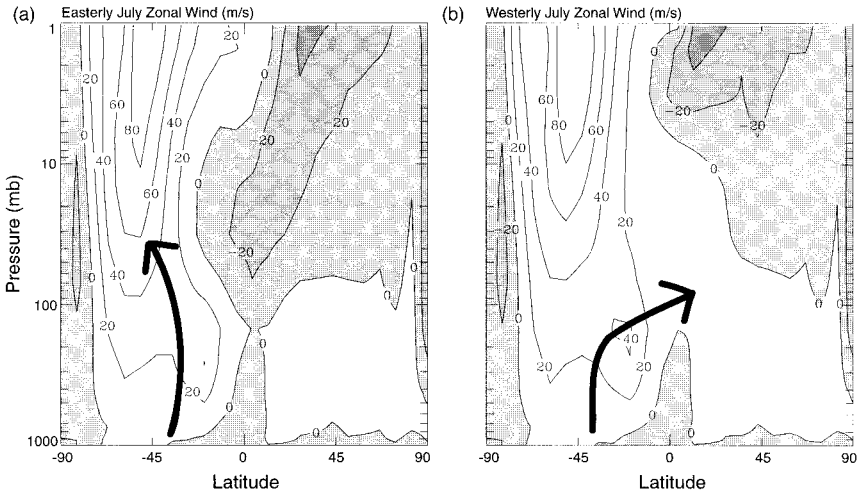

FIG. 5. Ten-year average zonal winds during July in the QBO easterly and westerly phases. The bold arrows indicate schematically the differences in wave propagation induced by the zonal wind and potential vorticity changes.

the same time, vertical propagation conditions are improved where the vorticity gradient has increased, with a net effect that tropospheric wave energy tends to reach the high-latitude stratosphere more effectively in the easterly phase, while it is able to travel to lower latitudes in the westerly phase (pictured schematically in Fig. 5). This agrees well with the greater refraction of wave energy toward high latitudes in easterly years seen by Hamilton (1989) and by Dunkerton and Baldwin (1991). The modeled variations are statistically significant, as shown in Table 2, which gives zonal mean forcing by EP flux divergence values for the three runs. The net result of variations in wave propagation is a midlatitude EP flux divergence forcing that is strongest in the easterly QBO phase and intermediate in the unforced case, while there is actually a slight negative forcing in the westerly QBO phase. Lower-stratospheric temperatures are significantly influenced by these flux divergence variations.

At the beginning of the austral spring, when sunlight returns to the polar region, we therefore find a relatively warm lower stratosphere and little active chlorine in the easterly phase of the QBO, an intermediate value in the unforced case, and the coldest temperatures and greatest amounts of active chlorine in the QBO westerly phase, consistent with the temperature changes shown in Fig. 2. In the presence of sunlight, active chlorine is continuously converted to chlorine monoxide, which then catalytically destroys ozone. The loss rate is proportional to the square of the abundance of chlorine mon-

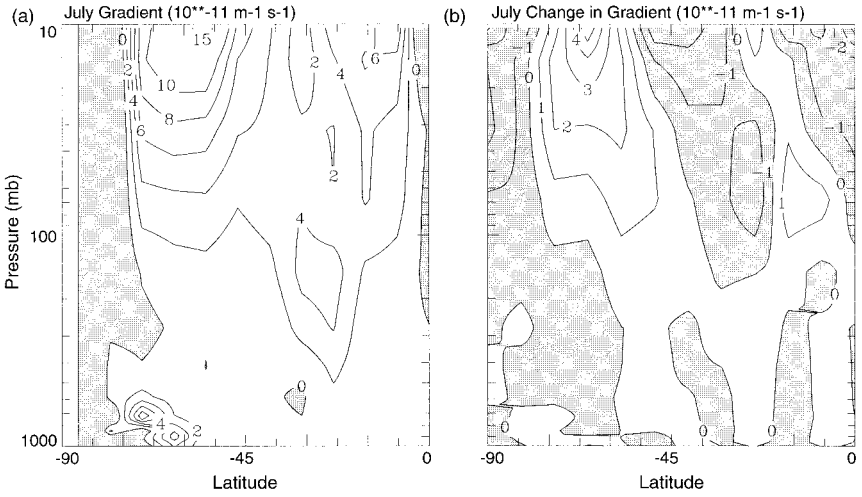

FIG. 6. Southern Hemisphere quasigeostrophic potential vorticity gradient in the easterly phase (left) and the gradient change between the easterly and westerly phase experiments (right). Values are 10-yr average zonal means for July.

oxide, so that significant differences in ozone depletion result from the differing levels of chlorine activation, as seen in Table 2. The temperature differences set up in July persist throughout the springtime period of ozone depletion, as was shown in Table 1, because the meridional wave propagation patterns that are set up are quite stable, with September flux divergence forcings similar to those shown in Table 2 for July. Springtime temperatures are positively correlated with midwinter wave activity and anticorrelated with EP flux divergence, which therefore leads to anticorrelations between total ozone loss and midwinter wave activity and between total ozone loss and EP flux divergence forcing of the zonal winds as shown in Table 2. To illustrate this point, total depleted ozone mass at the end of September, when ozone loss is near its maximum, is plotted against the July Southern Hemisphere tropospheric wave energy, against the July lower stratospheric EP flux divergence, and against the July zonal mean forcing by EP flux divergence for the 30 individual model years in Fig. 7. The QBO forcing extends the range of all three quantities, especially ozone loss, and the two QBO phases clearly have opposite effects. Based on a linear regression, the correlations of September ozone depletion with July Southern Hemisphere tropospheric wave energy is $R^2 = 0.42$ and with July lower stratospheric EP flux divergence is $R^2 = 0.58$. To the degree that they are independent variables, this indicates that the variations in EP flux divergence can explain roughly 50%–60% of the variability in the size of the ozone hole.

7. Discussion

A study of the relationship between the QBO and the severity of the Antarctic ozone hole was performed by Butchart and Austin (1996) using a three-dimensional mechanistic model (Austin and Butchart 1994). That model does not contain a troposphere, so that stratospheric dynamics are controlled by the imposed forcing at the model lower boundary (237.14 mb). Since there was no troposphere, interannual variability in the troposphere could not be included in their experiment.

They found that the QBO influenced the severity of the Antarctic ozone hole primarily through wave-induced modification of the transport circulation rather than through the temperature-dependent chemistry. However, their experiments covered only the time period from mid-August through November. Since there was no variability in the tropospheric forcing, the stratospheric temperatures were identical at the start of each run regardless of the QBO forcing. Significant temperature differences between the runs did not appear until late September, with large differences later on during October and November. Chlorine activation, and therefore chemical ozone depletion, was thus identical regardless of the QBO phase through late September in their experiments. This is in sharp contrast to our results, which included variability in midwinter wave energy forcing of the stratosphere, leading to appreciable temperature differences and, therefore, differences in chlorine activation levels between the QBO phases as early as July and August. Once sunlight returned to the Antarctic during early spring (late August to early September, depending on latitude), we therefore found distinct variations in chemical ozone depletion between the QBO easterly and westerly phases, especially near the edge of the ozone hole where chemical destruction began earliest. In an experiment that varied the wave forcing at the model lower boundary, Butchart and Austin did find an onset of temperature variability by the end of August. While their model lacks variability in tropospheric forcing, it treats both ozone transport and chemistry in a more sophisticated manner than that used in our study. Given those differences, the sensitivity of both transport and chemistry to the QBO is likely to differ somewhat between the models as well, making it is very difficult to account precisely for the discrepancies between the results.

8. Conclusions

To understand the relative impact of the QBO versus other natural variability on the severity of the ozone hole, we have performed GCM experiments both with and without a QBO forcing. In the unforced experiments, the differences in the amount of tropospheric wave energy in July and its subsequent propagation were correlated with temperatures and therefore, via chemistry, with ozone losses during August, September, and October, the key months for ozone hole formation. We find that the QBO forcing, even though applied only in the stratosphere, is able to modulate tropospheric wave energy amounts, causing more dynamical activity in the easterly phase than in the unforced case, while westerly phase years are dynamically more quiescent. More importantly, the QBO alters zonal winds and potential vorticity, increasing the effectiveness of wave energy propagation to high latitudes in the easterly phase while reducing it in the westerly phase. The net result is that zonal average temperatures in the Southern Hemisphere lower stratosphere are around 3–5 K warmer in the easterly maximum phase than in the westerly maximum during the winter and spring. These relatively small differences have a significant impact through the very nonlinear heterogeneous chemistry responsible for polar ozone depletion. The effect on the ozone hole can be clearly seen in the end of September mean total mass of ozone destroyed, which was 10.3×10^{10} kg in the unforced case, versus 8.7×10^{10} kg in the warmer easterly phase and 12.0×10^{10} kg in the cooler westerly phase. This loss is fairly well correlated with the midwinter EP flux divergence in the Southern Hemisphere lower stratosphere ($R^2 = 0.6$).

Without the QBO, natural variability in tropospheric wave energy propagation into the stratosphere led to a maximum variability of 3.3×10^9 kg in the mass of

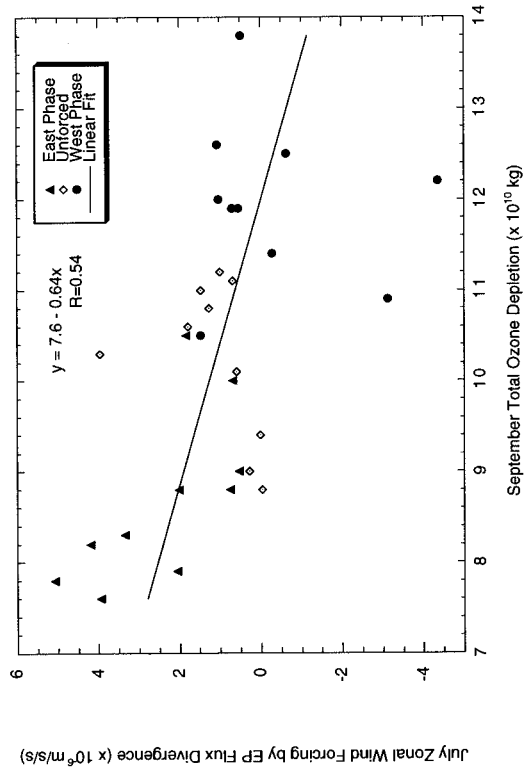

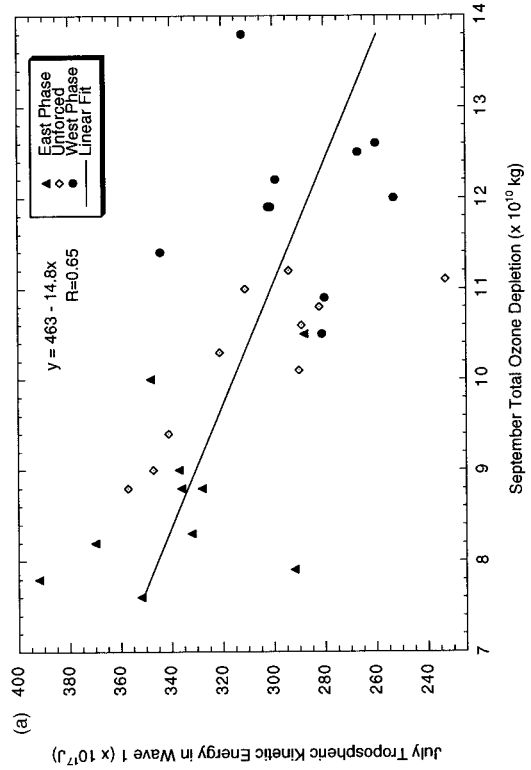

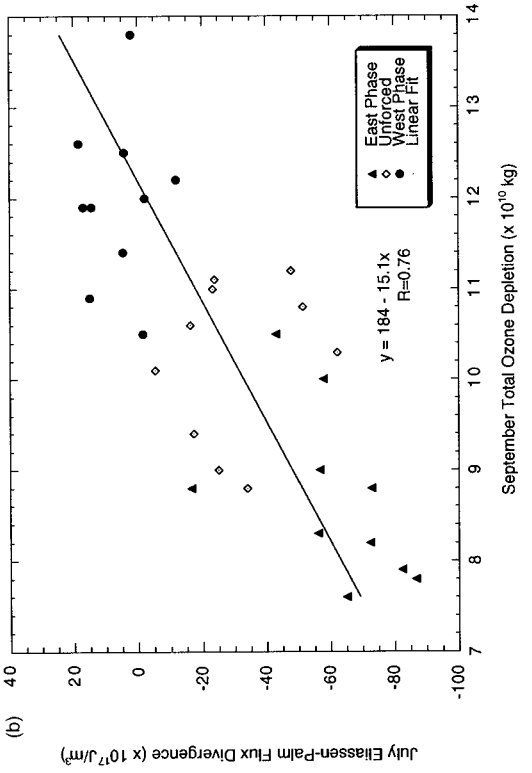

FIG. 7. Scatterplots showing the correlation between total ozone depletion at the end of September and midwinter tropospheric wave energy (upper left panel), Jul EP flux divergence (upper right panel), following convention, values that are more negative indicate grater divergence, and Jul zonal wind forcing by EP flux divergence (bottom left panel), 30 individual years of model experiments. Ten years each are shown for the QBO easterly phase, the QBO westerly phase, and the unforced case. Model ozone losses are totals, not only those at latitudes less than 70°S and with column ozone below 220 DU, as was done for comparison with the analysis of TOMS observations. The EP flux divergences and zonal wind accelerations by EP flux divergence forcing are mean values for 23°–55°S, from 10 to 150 mb. The lines are linear regression fits to the data, with the line formulas and correlation coefficients as indicated.

ozone depleted, with a standard deviation of 1.2×10^9 kg, for the subset of model results corresponding to the times and locations of TOMS observations. When the QBO forcing was applied at a constant maximum value, the largest variations in the same subset of ozone losses increased to 9.8×10^9 kg. The QBO-induced variations are much closer to the maximum variations of 7.4×10^9 kg observed by TOMS. The model results suggest that unforced variability is responsible for roughly one-third of the variations in ozone hole depth, while the QBO forcing is responsible for roughly two-thirds based on a comparison of the maximum variations induced in each experiment. The impact of additional potential influences on the ozone hole, such as solar variability, volcanoes, or the El Niño–Southern Oscillation, remains to be studied.

Acknowledgments. Support was provided by NASA's Atmospheric Chemistry Modeling and Analysis Program and NSF Solar Terrestrial Physics Grant ATM 95-23326. Thanks to Jean Lerner for graphics, Patrick Lonergan for GCM runs, Steven Pawson for providing the updated equatorial winds, Rich McPeters for information on TOMS data, and Greg Bodeker for providing the yearly ozone depletion values.

REFERENCES

Austin, J., and N. Butchart, 1994: The influence of climate change and the timing of stratospheric warmings on Arctic ozone depletion. *J. Geophys. Res.,* **99,** 1127–1145.

Balachandran, N., and D. Rind, 1995: Modeling the effects of UV variability and the QBO on the troposphere–stratosphere system. Part I: The middle atmosphere. *J. Climate,* **8,** 2058–2079.

Bodeker, G. E., and M. W. J. Scourfield, 1995: Planetary waves in total ozone and their relation to Antarctic ozone depletion. *Geophys. Res. Lett.,* **22,** 2949–2952.

Bojkov, R. D., 1986: The 1979–1985 ozone decline in the Antarctic as reflected in ground-based observations. *Geophys. Res. Lett.,* **13,** 1236–1239.

Butchart, N., and J. Austin, 1996: On the relationship between the quasi-biennial oscillation, total chlorine and the severity of the Antarctic ozone hole. *Quart. J. Roy. Meteor. Soc.,* **122,** 183–217.

Cariolle, D., A. Lasserre-Bigorry, J.-F. Royer, and J.-F. Geleyn, 1990: A general circulation model simulation of the springtime Antarctic ozone decrease and its impact on mid-latitudes. *J. Geophys. Res.,* **95,** 1883–1898.

Dameris, M., V. Grewe, R. Hein, C. Schnadt, C. Bruhl, and B. Steil, 1998: Assessment of the future development of the ozone layer. *Geophys. Res. Lett.,* **25,** 3579–3582.

Dunkerton, T. J., and M. P. Baldwin, 1991: Quasi-biennial modulation of planetary wave fluxes in the Northern Hemisphere winter. *J. Atmos. Sci.,* **48,** 1043–1061.

Garcia, R. R., and S. Solomon, 1987: A possible relationship between interannual variability in Antarctic ozone and the quasi-biennial oscillation. *Geophys. Res. Lett.,* **14,** 848–851.

Gray, L. J., and S. Ruth, 1993: The modeled latitudinal distribution of the ozone quasi-biennial oscillation using observed equatorial winds. *J. Atmos. Sci.,* **50,** 1033–1046.

Hamilton, K., 1989: Interhemispheric asymmetry and annual synchronization of the ozone quasi-biennial oscillation. *J. Atmos. Sci.,* **46,** 1019–1025.

——, 1995: Comprehensive simulation of the middle atmosphere climate—Some recent results. *Climate Dyn.,* **11,** 223–241.

Hasebe, F., 1983: Interannual variations of global ozone revealed from NIMBUS 4 BUV and ground based observations. *J. Geophys. Res.,* **88,** 6819–6834.

Hess, P. G., and D. O'Sullivan, 1995: A three-dimensional modeling study of the extratropical quasi-biennial oscillation in ozone. *J. Atmos. Sci.,* **52,** 1539–1554.

Holton, J. R., and H.-C. Tan, 1980: The influence of the equatorial quasi-biennial oscillation on the global circulation at 50 mb. *J. Atmos. Sci.,* **37,** 2200–2208.

Jaeglé, L., and Coauthors, 1997: Evolution and stoichiometry of heterogeneous processing in the Antarctic stratosphere. *J. Geophys. Res.,* **102,** 13 235–13 253.

Kodera, K., 1991: The solar and equatorial QBO influences on the stratospheric circulation during the early northern-hemisphere winter. *Geophys. Res. Lett.,* **18,** 1023–1026.

Lait, L. R., M. R. Schoeberl, and P. A. Newman, 1989: Quasi-biennial modulation of the Antarctic ozone depletion. *J. Geophys. Res.,* **94,** 11 559–11 571.

McPeters, R., and Coauthors, 1996: Long-term trends derived from the 16-year combined Nimbus 7/Meteor 3 TOMS version 7 record. *Geophys. Res. Lett.,* **23,** 3699–3702.

Naujokat, B., 1986: An update of the observed quasi-biennial oscillation of the stratospheric winds over the Tropics. *J. Atmos. Sci.,* **43,** 1873–1877.

Prather, M., and A. H. Jaffe, 1990: Global impact of the Antarctic ozone hole: Chemical propagation. *J. Geophys. Res.,* **95,** 3473–3492.

Randel, W. J., 1987: Global atmospheric circulation statistics, 1000-1 mb. NCAR Tech. Note NCAR/TN-295+STR, 245 pp.

Rind, D., R. Suozzo, N. K. Balachandran, A. Lacis, and G. Russell, 1988a: The GISS global climate/middle atmosphere model. Part I: Model structure and climatology. *J. Atmos. Sci.,* **45,** 329–370.

——, ——, and ——, 1988b: The GISS global climate/middle atmosphere model. Part II: Model variability due to interactions between planetary waves, the mean circulation, and gravity wave drag. *J. Atmos. Sci.,* **45,** 371–386.

Shindell, D. T., and R. L. de Zafra, 1997: Limits on heterogeneous processing in the Antarctic spring vortex from a comparison of measured and modeled chlorine. *J. Geophys. Res.,* **102,** 1441–1450.

——, S. Wong, and D. Rind, 1997: Interannual variability of the Antarctic ozone hole in a GCM. Part I: The influence of tropospheric wave variability. *J. Atmos. Sci.,* **54,** 2308–2319.

——, D. Rind, and P. Lonergan, 1998a: Increased polar stratospheric ozone losses and delayed eventual recovery due to increasing greenhouse gas concentrations. *Nature,* **392,** 589–592.

——, ——, and ——, 1998b: Climate change and the middle atmosphere. Part IV: Ozone photochemical response to doubled CO_2. *J. Climate,* **11,** 895–918.

Stolarski, R. S., A. J. Krueger, M. R. Schoeberl, R. D. McPeters, P. A. Newman, and J. C. Alpert, 1986: Nimbus 7 satellite measurements of the springtime Antarctic ozone decrease. *Nature,* **322,** 808–811.

World Meteorological Organization, 1994: Scientific assessment of ozone depletion. Rep. 37, Global Ozone Research and Monitoring Project, 541 pp.